Available online at www.sciencedirect.com
ScienceDirect
Nuclear and Particle Physics Proceedings 00 (2015) 1–5
Nuclear and Particle Physics Proceedings

Application of AdS/QCD to B physics

Mohammad Ahmady[a,1], Sébastien Lord[b,**], Ruben Sandapen[a,c]

[a] *Department of Physics, Mount Allison University, Sackville, New Brunswick, Canada E4L 1E6*
[b] *Département de Mathématiques et Statistique, Université de Moncton, Moncton, New Brunswick, Canada E1A 3E9*
[c] *Department of Physics, Acadia University, Wolfville, Nova-Scotia, Canada, B4P 2R6*

Abstract

We build on the success of AdS/QCD in predicting diffractive ρ meson production to obtain the transition form factors for B decays to light mesons. Consequently, we predict several observables associated with $B \to \rho \ell \nu$ semileptonic and $B \to K^* \mu^+ \mu^-$ dileptonic decays. Our predictions are compared to the available experimental data.

Keywords: Rare B meson decays, distributions amplitudes, AdS/QCD, light-cone sum rules

1. Introduction

Rare B meson decays are excellent venues for precision test of the standard model (SM) and search for new physics (NP) beyond it. The underlying quark processes for these decays are suppressed either due to small Cabbibo-Kobayashi-Mashawa (CKM) quark mixing or lack of flavor changing neutral current (FCNC) at tree level in SM. For example, the semileptonic $B \to \rho \ell \nu$ decay can help with our knowledge of the least known CKM matrix element V_{ub}. On the other hand, a rare B decay like $B \to K^* \mu^+ \mu^-$ occurs only through quantum loops, and is sensitive to new unknown particles that are predicted by various NP scenarios beyond the SM. These so-called exotic particles can appear as virtual entries in the loops and alter the decay rate and other associated observables from what is expected within the SM. This indirect search for NP in rare B meson decays has been used to constrain various scenarios like supersymmetry and vector-like quark model.

In this talk, we report on a number of predictions for semileptonic $B \to \rho \ell \nu$ and dileptonic $B \to K^* \mu^+ \mu^-$ decays based on the anti-de Sitter/Quantum Chromodynamics (AdS/QCD)[1, 2]. The holographic light-front wavefunctions obtained from AdS/QCD are used to calculate the distribution amplitudes (DAs) of the ρ and K^* vector mesons[3, 4]. These DAs are then inserted in light-cone sum rules (LCSR) formulas for $B \to \rho,\ K^*$ transition form factors[5, 6, 7].

2. Transition form factors

The nonperturbative QCD effects appear in the $B \to V,\ V = \rho,\ K^*$ transition matrix elements which are parametrized in terms of a number of form factors. Understanding these form factors is crucial in theoretical calculation of the exclusive B meson decays to light mesons. Some or all of the 7 form factors defined below appear in semileptonic or dileptonic B decays:

$$\begin{aligned}
&\langle V(k,\varepsilon)|\bar{q}\gamma^\mu(1-\gamma^5)b|B(p)\rangle \\
&= \frac{2iV(q^2)}{m_B + m_{K^*}} \epsilon^{\mu\nu\rho\sigma} \varepsilon^*_\nu k_\rho p_\sigma - 2m_{K^*} A_0(q^2) \frac{\varepsilon^* \cdot q}{q^2} q^\mu \\
&- (m_B + m_{K^*}) A_1(q^2) \left(\varepsilon^{\mu *} - \frac{\varepsilon^* \cdot q q^\mu}{q^2} \right) \\
&+ A_2(q^2) \frac{\varepsilon^* \cdot q}{m_B + m_{K^*}} \left[(p+k)^\mu - \frac{m_B^2 - m_{K^*}^2}{q^2} q^\mu \right]
\end{aligned}$$

*Talk given at 18th International Conference in Quantum Chromodynamics (QCD 15, 30th anniversary), 29 june - 3 july 2015, Montpellier - FR

**Senior undergraduate student.

Email addresses: mahmady@mta.ca (Mohammad Ahmady), esl8420@umoncton.ca (Sébastien Lord), rsandapen@mta.ca (Ruben Sandapen)

[1] Speaker, Corresponding author.

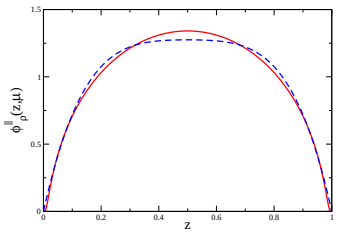

(a) Twist-2 DA for the longitudinally polarized ρ meson

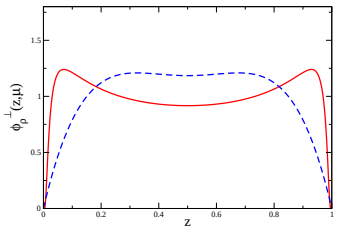

(b) Twist-2 DA for the transversely polarized ρ meson

Figure 1: Twist-2 DAs for the ρ meson. Solid: AdS/QCD DAs; Dashed: Sum Rules DAs.

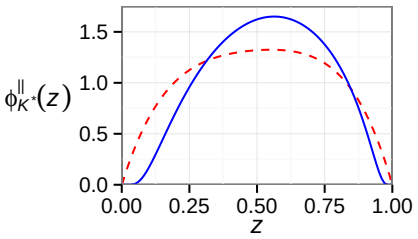

(a) Twist-2 DA for the longitudinally polarized K^* meson

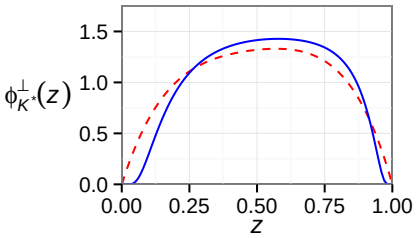

(b) Twist-2 DA for the transversely polarized K^* meson

Figure 2: Twist-2 DAs for the K^* meson. Solid: AdS/QCD DAs; Dashed: Sum Rules DAs.

$$
\begin{aligned}
&q_\nu\langle V(k,\varepsilon)|\bar{q}\sigma^{\mu\nu}(1-\gamma^5)b|B(p)\rangle \\
&= 2T_1(q^2)\epsilon^{\mu\nu\rho\sigma}\varepsilon^*_\nu p_\rho k_\sigma \\
&- iT_2(q^2)[(\varepsilon^*\cdot q)(p+k)_\mu - \varepsilon^*_\mu(m_B^2 - m_{K^*}^2)] \\
&- iT_3(q^2)(\varepsilon^*\cdot q)\left[\frac{q^2}{m_B^2 - m_{K^*}^2}(p+k)_\mu - q_\mu\right] \qquad (1)
\end{aligned}
$$

We use LCSR[8, 9] to calculate the seven form factors in terms of the DAs of the light vector mesons. LCSR are variations of the traditional QCD Sum Rules whereby non-local matrix elements are expanded in terms of light front DAs. Using light-cone coordinates, $x^\pm = x^0 \pm x^3$, $x^\perp = x^1,\ x^2$, the two twist-2 DAs $\phi_{\perp,\parallel}$ along with the two twist-3 DAs $g_\perp^{(v,a)}$ are defined through the following relations[10]:

$$
\begin{aligned}
&\langle 0|\bar{q}(0)\gamma^\mu q(x^-)|V(P,\lambda)\rangle \\
&= f_V M_V \frac{e_\lambda\cdot x}{P^+x^-}P^\mu\int_0^1 \mathrm{d}u\ e^{-iuP^+x^-}\phi_\parallel(u,\mu) \\
&+ f_V M_V\left(e^\mu_\lambda - P^\mu\frac{e_\lambda\cdot x}{P^+x^-}\right)\int_0^1 \mathrm{d}u\ e^{-iuP^+x^-}g_\perp^{(v)}(u,\mu)\ , \\
&\langle 0|\bar{q}(0)[\gamma^\mu,\gamma^\nu]q(x^-)|V(P,\lambda)\rangle \\
&= 2f_V^\perp(e^\mu_\lambda P^\nu - e^\nu_\lambda P^\mu)\int_0^1 \mathrm{d}u\ e^{-iuP^+x^-}\phi_\perp(u,\mu)\ , \\
&\langle 0|\bar{q}(0)\gamma^\mu\gamma^5 s(x^-)|V(P,\lambda)\rangle \\
&= -\frac{1}{4}\epsilon^\mu_{\nu\rho\sigma}e^\nu_\lambda P^\rho x^\sigma \tilde{f}_V M_V\int_0^1 \mathrm{d}u\ e^{-iuP^+x^-}g_\perp(a)(u,\mu)\ ,
\end{aligned}
\qquad (2)
$$

where

$$\tilde{f}_\rho = f_\rho\ , \qquad (3)$$

and

$$\tilde{f}_{K^*} = f_{K^*} - f_{K^*}^\perp\left(\frac{m_s + m_{\bar{q}}}{M_{K^*}}\right)\ . \qquad (4)$$

m_s and $m_{\bar{q}}$ are the masses of the strange quark and light anti-quark, respectively. Also, all the above-defined DAs are normalized, i.e.

$$\int_0^1 \mathrm{u}\ \phi_V^{\perp,\parallel}(u,\mu) = \int_0^1 \mathrm{u}\ g_V^{\perp(a,v)}(u,\mu) = 1$$

As $x^- \to 0$, in Eqn. 2 we recover the usual definition for the decay constant f_V and $f_V^\perp$:

$$\langle 0|\bar{q}(0)\gamma^\mu q(0)|V(P,\epsilon)\rangle = f_V M_V\epsilon^\mu\ , \qquad (5)$$

$$\langle 0|\bar{q}(0)[\gamma^\mu,\gamma^\nu]q(0)|V(P,\epsilon)\rangle = 2f_V^\perp(\epsilon^\mu P^\nu - \epsilon^\nu P^\mu)\ . \qquad (6)$$

The DAs which are commonly used in the literature are derived from QCD sum rules (SR). In the next section, we put forward alternative DAs which are obtained from AdS/QCD.

3. AdS/QCD holographic DAs

The holographic light-front wavefunction for a vector meson ($L = 0, S = 1$) in AdS/QCD can be written as[1, 11]:

$$\begin{aligned}\phi_\lambda(z,\zeta) &= \mathcal{N}_\lambda \sqrt{z(1-z)}\exp\left(-\frac{\kappa^2\zeta^2}{2}\right)\\ &\times \exp\left\{-\left[\frac{m_q^2 - z(m_q^2 - m_{\bar{q}}^2)}{2\kappa^2 z(1-z)}\right]\right\} \qquad (7)\end{aligned}$$

with $\kappa = M_V/\sqrt{2}$ and $m_q = m_{\bar{q}}$ or m_s for ρ or K^* respectively. λ is the polarization of the vector meson. We have introduced the dependence on quark masses following a prescription by Brodsky and de Téramond [11]. This wavefunction for the ρ meson was successfully used to predict diffractive ρ meson electroproduction at HERA[12].

The relation between the wavefunction (7) and DAs for ρ and K^* was derived in [3, 4]. Figures 3 and 2 compare the two twist-2 DAs for these two vector mesons obtained from AdS/QCD and SR.

Consequently, the AdS/QCD predictions for $B \to \rho$, K^* form factors can be computed via LCSR. One should note that LCSR results are valid at low to intermediate values of the momentum transfer q^2. Figure 4 illustrates the AdS/QCD predictions for two $B \to \rho$ form factors V and T_1 when 3 different values of the quark mass are used. Our results for the all 7 form factors for this transition can be found in [5]. The data points on this figure are from lattice calculation which are available at high q^2[13]. To calculate the differential branching of the semileptonic $B \to \rho\ell\nu$ decay, we find two-parameter fits for the form factors using AdS/QCD predictions at low to intermediate q^2 and lattice data at high q^2[5].

Figure 5 shows the AdS/QCD prediction for $B \to K^*$ form factors V and T_1 as compared with those obtained from SR. The data points at high q^2 are from lattice calculations[14]. Our results for the full set of $B \to K^*$ transition form factors can be found in [6]. Similar to $B \to \rho$ case, we use two-parameter fits to AdS/QCD and lattice data combined for the form factors and use them in our numerical computations.

4. Numerical predictions for observables

The differential decay rate of the semileptonic $B \to \rho\ell\nu$ is sensitive to V_{ub}. Figure 3 shows our AdS/QCD prediction for the differential decay rate divided by $|V_{ub}|^2$ for two different quark masses. The data points on this figure are lattice predictions generated by UKQCD Collaboration[13].

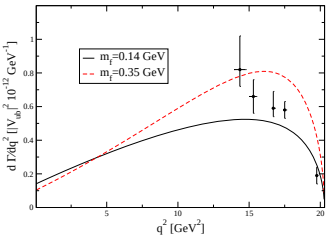

Figure 3: Differential decay rate for the semileptonic $B \to \rho\ell\bar{\nu}$ decay. The lattice data points are from UKQCD Collaboration.

BaBar collaboration has measured the partial branching fractions for this decay channel in three q^2 bins[15]: $\Delta B_{\rm low} = (0.564 \pm 0.166) \times 10^{-4}$, $\Delta B_{\rm mid} = (0.912 \pm 0.147) \times 10^{-4}$ and $\Delta B_{\rm high} = (0.268 \pm 0.062) \times 10^{-4}$ for $0 < q^2 < 8$, $8 < q^2 < 16$ and $16 < q^2 < 20.3$ GeV^2 respectively. To eliminate the uncertainty in V_{ub} when comparing our results with the above data, we take the ratios of the partial branching fractions as defined below:

$$\begin{aligned}R_{\rm low} &= \frac{\Delta B_{\rm low}}{\Delta B_{\rm mid}} = 0.618 \pm 0.207\ ,\\ R_{\rm high} &= \frac{\Delta B_{\rm high}}{\Delta B_{\rm mid}} = 0.294 \pm 0.083\ . \qquad (8)\end{aligned}$$

Our AdS/QCD predictions for these ratios are $R_{\rm low} = 0.580, 0.424$ and $R_{\rm high} = 0.427, 0.503$ for $m_q = 0.14$ GeV, 0.35 GeV. It seems that better agreement with data is achieved at low q^2.

Our results for the differential branching ratio and isospin asymmetry distribution in $B \to K^*\mu^+\mu^-$ are shown in Figure 6. Data points for the branching ratio are from LHCb[16] and the prediction is given with (solid curve) and without (dashed curve) the $c\bar{c}$ resonance contributions. Our AdS/QCD prediction for the isospin asymmetry distribution in $B \to K^*\mu^+\mu^-$ in Figure 6 is presented (solid curve) with an uncertainty band due to the renormalization scale variation from $m_b/2$ to $2m_b$. The data points are from LHCb and PDG[17, 18]. For comparison, we also include the SR predictions (dashed curve) for isospin asymmetry distribution. Our prediction for asymmetry at $q^2 = 0$ (relevant to $B \to K^*\gamma$) is consistent with experimental data.

5. Acknowledgements

This research is supported by a team grant from the Natural Sciences and Engineering Research Council of

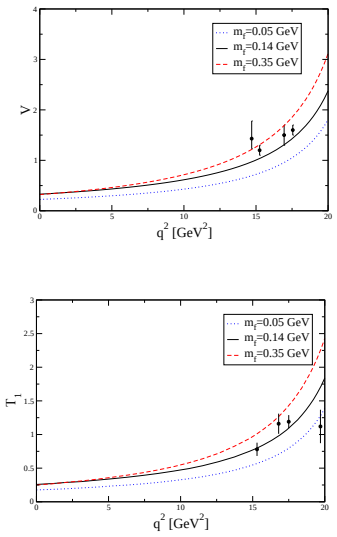

Figure 4: The AdS/QCD prediction for $B \to \rho$ transition form factors V and T_1 for 3 different quark mass inputs. The available lattice data at high q^2 are shown as well.

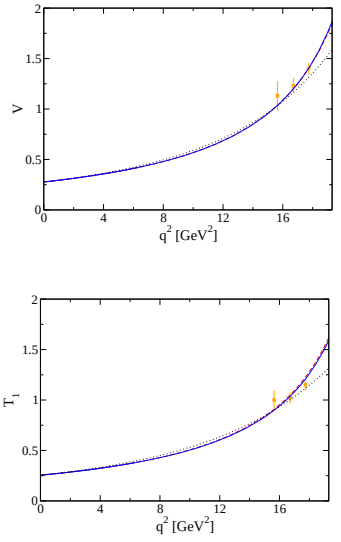

Figure 5: The AdS/QCD prediction for $B \to K^*$ transition form factors V and T_1. The solid curve denotes AdS/QCD. The dashed curve denotes the AdS/QCD fit. The dotted curve denotes the fit to AdS/QCD and lattice. The available lattice data at high q^2 are shown as well.

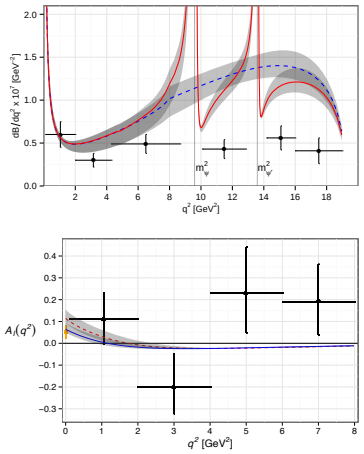

Figure 6: The AdS/QCD prediction for $B \to K^*\mu^+\mu^-$ differential branching ratio and isospin asymmetry distribution. The differential branching ratio is predicted with (solid curve) and without (dashed curve) $c\bar{c}$ resonances. In the isospin asymmetry graph, AdS/QCD prediction (solid curve) is presented with an uncertainty band and compared with SR expectation (dashed curve).

Canada (NSERC). SL thanks the government of New-Brunswick for SEED-COOP funding.

References

[1] G. F. de Téramond and S. J. Brodsky, Phys. Rev. Lett. 102, 081601 (2009).
[2] S.J. Brodsky, G.F. de Teramond, H.G. Dosch, and J. Erlich, Phys. Rep. **584**, 1 (2015).
[3] M. Ahmady and R. Sandapen, Phys.Rev. D 88 054013 (2013).
[4] M. Ahmady and R. Sandapen, Phys. Rev. D 88 014042 (2013).
[5] M. Ahmady, R. Campbell, R. Sandapen, and S. Lord, Phys. Rev. D 88 074031 (2013).
[6] M. Ahmady, R. Campbell, S. Lord, and R. Sandapen, Phys. Rev. D 89 014042 (2014).
[7] M. Ahmady, S. Lord, and R. Sandapen, Phys. Rev. D 90 074010 (2014).
[8] A. Ali, V. M. Braun, and H. Simma, Z. Phys. C 63, 437 (1994).
[9] P. Ball and V. M. Braun, Phys. Rev. D 55, 5561 (1997); P. Ball and V. M. Braun, Phys. Rev. D 58, 094016 (1998); P. Ball and R. Zwicky, Phys. Rev. D 71, 014029 (2005); T. Aliev, A. Ozpineci, and M. Savci, Phys. Rev. D 56, 4260 (1997).
[10] P. Ball, V. M. Braun, and A. Lenz, J. High Energy Phys. 08, 090 (2007).
[11] S. J. Brodsky and G. F. de Teramond, AIP Conf. Proc. 1116, 311 (2009).
[12] J. R. Forshaw and R. Sandapen, Phys. Rev. Lett. 109, 081601 (2012).
[13] D. R. Burford, H. D. Duong, J. M. Flynn, B. J. Gough, N. M. Hazel, J. Nieves, and H. P. Shanahan (UKQCD Collaboration), Nucl. Phys. 447 425 (1995); J. M. Flynn, arXiv:hep-lat/9611016; L. Del Debbio, J. M. Flynn, L. Lellouch, and J. Nieves (UKQCD Collaboration), Phys. Lett. B 416 392 (1998).
[14] R. R. Horgan, Z. Liu, S. Meinel, and M. Wingate, Phys. Rev. D 89 094501 (2014).

[15] P. del Amo Sanchez et al. (BABAR Collaboration), Phys. Rev. D 83 032007 (2011).
[16] T. Blake and N. Serra (LHCb Collaboration) Report No. CERN-LHCb-CONF-2012-008; R. Aaij et al. (LHCb Collaboration), J. High Energy Phys. 07 133 (2012).
[17] R. Aaij et al. (LHCb collaboration), J. High Energy Phys. 06 133 (2014).
[18] J. Beringer et al. (Particle Data Group), Phys. Rev. D 86, 010001 (2012).